Mathematical Biosciences and Engineering

http://www.aimspress.com/journal/MBE

MBE, 17(6): 7645–7670.
DOI: 10.3934/mbe.2020389
Received: 29 June 2020
Accepted: 11 October 2020
Published: 04 November 2020

Research article

Dynamics of competing heterogeneous clones in blood cancers explains multiple observations - a mathematical modeling approach

Katrine O. Bangsgaard[1], Morten Andersen[1], Vibe Skov[2], Lasse Kjær[2], Hans C. Hasselbalch[2] and Johnny T. Ottesen[1,*]

[1] IMFUFA, Department of Science and Environment, Roskilde University, Roskildevej 1, DK 4000, Denmark

[2] Department of Hematology, Zealand University Hospital, Sygehusvej 10, DK 4000, Denmark

* **Correspondence:** Email: johnny@ruc.dk.

Supplementary

S.1. The Multiple Clone Cancitis Model

Inspired by clinical observations the MCC model has been formulated in attempt to gain an understanding of the more complex dynamics such as resistance and oscillations.

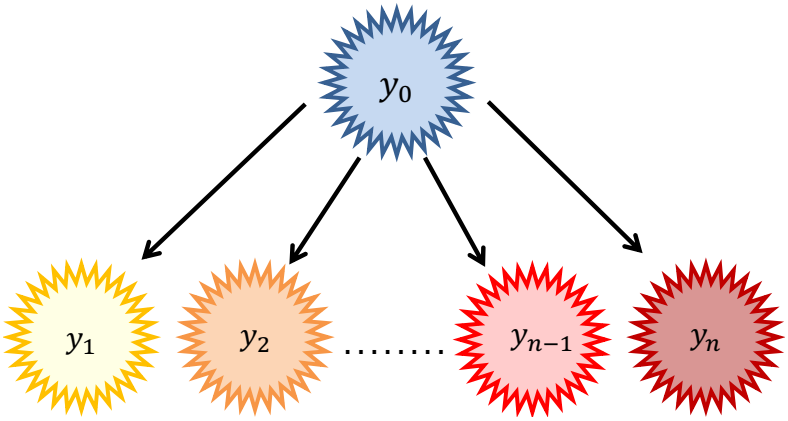

Figure S.1. Conceptual diagram for the parallel mutations. The WSCs (y_0) have the possibility to mutate into n types of mutated stem cells ($y_1, y_2, \ldots, y_n$).

Mutations can occur in the WSCs but the MSCs can themselves also mutate. Here we will consider the two limits, either the WSCs mutate into different MSCs (parallel mutation), or the WSCs mutates into a single mutated stem cell which initiate a sequence of mutations (sequential mutation).

A conceptual diagram of the parallel mutation is depicted in Figure S.1. The diagram illustrates how the healthy stem cells have probability to mutate into several malignant stem cell types and thereby giving rise to the concept of cancer heterogeneity. Cancer heterogeneity can also be viewed as arising through a sequential mutation process and an aggressive malignant cell type is likely to arise from such a sequence of mutations. The sequential mutations are illustrated in Figure S.2, where the healthy stem cells mutate into a posibly malignant cell type, which itself may mutate further and so on a number of times n.

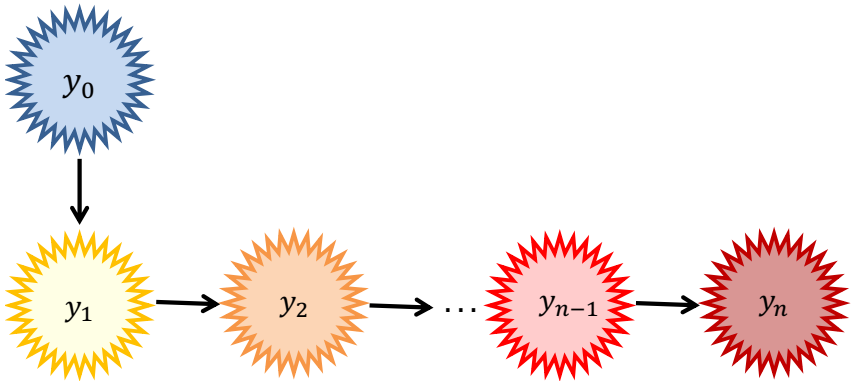

Figure S.2. Conceptual diagram for sequential mutations. The wild type stem cells (y_0) may mutate to y_1 and y_1 then starts a sequence of mutations.

Each cell after multiple mutations may be a result of the mutations arriving in any order, thus resulting in cells with equivalent DNA. However, the histology of the cells may differ causing the cells to be phenomenologically different. Due to this phenomena a very large class of mutational landscapes are possible. In simulations we may randomly chose an existing cell to mutate and randomly chose the type of mutation (parallel or sequential) in each sufficiently small time intervals. Doing a Monte Carlo simulation of such random process would give information about mean and variation but less mechanistic insight.

In this paper we present a parallel MCC model and a sequential MCC model, allowing for parallel mutations and sequential mutations, respectively. The two versions represent two limit cases of the possible mutational landscape, thus we chose to study these and amazingly the two limit cases result in very similar outcome in almost all cases. Further, with stochastic mutation between stem cell clones intermediate cases are also covered.

S.1.1. The equations of the parallel Multiple Clone Cancitis Models

Let y_0 and z_1 denote the amount of wild type WSCs and the mature blood cells, respectively. Let the amount of the i'th mutated stem cell type be denoted y_i and let the amount of the corresponding i'th mature cell from this cell line be denoted z_i. Moreover, let the variable a denote the amount of death cells. The immune response is lumped into the variable s with the exception of the CD8+ T-cells as their effect is included explicitly in the model [1], which we adopt here in all the presented models.

A mathematical model for the cancer heterogeneity caused by parallel mutations in MPNs may be formulated as

$$\dot{y}_0 = \left(r_0\varphi_0 s - d_{y_0} - a_0\right) y_0 + \xi_0, \tag{S.1a}$$

$$\dot{y}_i = (r_i\varphi_i s - d_{y_i} - \tilde{d}_{y_i} y_i - a_i) y_i + \xi_i, \quad \text{for} \quad i = 1, 2, \ldots, n, \tag{S.1b}$$

$$\dot{z}_i = a_i A_i y_i - d_{z_i} z_i, \qquad \text{for} \quad i = 0, 1, \ldots, n, \tag{S.1c}$$

$$\dot{a} = d_{y_0} y_0 + d_{z_0} z_0 + \sum_{j=1}^{n} \left(\left(d_{y_j} + \tilde{d}_{y_j} y_j\right) y_j + d_{z_j} z_j\right) - e_a s a, \tag{S.1d}$$

$$\dot{s} = r_s a - e_s s + I, \tag{S.1e}$$

where n being the number of malignant clones. The constant r_i is the self-renewal rate for the stem cells type i, d_{y_i}, d_{z_i} are the natural death rates, $\tilde{d}_{y_i}$ is the T-cell dependent death rate for the malignant stem cells. The constants a_i describe the rates which stem cells proliferate into progenitor cells whereas A_i are the amplification factors for which progenitor cells proliferate into mature cells by help of the intermediate proliferative progenitor cells. Here $\xi_i = \sum_{j=1}^{n} \xi_{j,i} - \xi_{i,j}$, where $\xi_{i,j}$ represent a stochastic mutational process for cell type j to cell type i. In the continuous limit $\xi_{j,i} = m_{j,i} y_i$, where the constant $m_{j,i}$ describe the probability for y_i to mutate into a malignant stem cell of type y_j corresponding to a continuous mutation rate. In the stochastic case the mutation process is a a Poisson process. The parameter r_s is the rate for which the number of dead cells up regulates the immune response, e_s is the elimination rate for the inflammatory level and I is an exogenous stimuli of the immune response relative to the system of stem cells, e.g. chronic inflammation, smoking, pollution or obesity [2, 3]. Lastly, the $\varphi_i = \varphi_i(y_0, y_1, ..., y_n)$ are functions describing the inhibiting bone marrow niche feedback from all stem cells onto cell type i, which is explicitly specified below. Default values for the model in the case of JAK2$^+$ MPNs can be found in Table A1.

Note that one could include several levels of progenitor cells between stem cells and mature cells, e.g. introducing equations for the progenitor cells, let $y_{i,0}$ and $y_{i,p}$ denote the stem cells and mature cells,respectively and let the progenitor cells be denoted by $y_{i,j}$ for $j = 1, 2, \ldots, p-1$. The differential equations for the progenitor cells are given by

$$\begin{aligned}
\dot{y}_{i,1} &= a_{i,0} y_{i,0} - d_{y_{i,1}} y_{i,1} \\
&\vdots \\
\dot{y}_{i,p} &= a_{i,p-1} y_{i,p-1} - d_{y_{i,p}} y_{i,p}
\end{aligned}$$

However, a quasi steady state approximation (QSSA) implies

$$y_{i,p} = \frac{a_{i,p-1}}{d_{y_{i,p}}} y_{i,p-1} = \ldots = \left(\prod_{j=1}^{p} \frac{a_{i,j-1}}{d_{y_{i,j}}}\right) y_{i,1} \equiv A_i y_{i,0}.$$

Thus the final amount of mature cells may be found by the amount of WSCs multiplied by a suitable factor describing the amplification factor.

The MCC model is brought into dimensionless form in order to reduce the dimension of the model as well as the number of free parameters. The derivation of the reduced MCC model follows the approach proposed in [1]. The dimensionless variables are denoted by capital letters and the scaling constants are denoted by the same symbols as the corresponding original variable with a bar, as an example the WSC compartment (y_0) can be expressed by $y_0 = \bar{y}_0 Y_0$ where Y_0 is the dimensionless variable and $\bar{y}_0$ is a constant carrying units. The corresponding derivative of y_0 with respect to the dimensionless time T can be expressed

$$\dot{y}_0 = \frac{\bar{y}_0}{\bar{t}} Y_0',$$

with $Y_0' = \frac{\mathrm{d}}{\mathrm{d}T} Y_0$ where $\bar{t}$ carries the unit with respect to time. Thus the continuous MCC model can be expressed by

$$\begin{aligned}
Y_0' &= \bar{t}\left(\left(\bar{s} r_0 \varphi_0 S - d_{y_0} - a_0\right) Y_0 + \frac{\xi_0}{\bar{y}_0}\right),\\
Y_i' &= \bar{t}\left(\left(\bar{s} r_i \varphi_i S - \hat{d}_{y_i}(Y_i) - a_i\right) Y_i + \frac{\xi_i}{\bar{y}_i}\right),\\
Z_i' &= \bar{t}\left(\frac{\bar{y}_i}{\bar{z}_i} a_i A_i Y_i - d_{z_i} Z_i\right),\\
A' &= \bar{t}\left(d_{y_0}\frac{\bar{y}_0}{\bar{a}} Y_0 + d_{z_0}\frac{\bar{z}_0}{\bar{a}} Z_0 - e_a \bar{s} S A + \sum_{j=1}^{n} \frac{\bar{y}_j}{\bar{a}} \hat{d}_{y_j}(Y_j) + \frac{\bar{z}_j}{\bar{a}} d_{z_j} Z_j\right),\\
S' &= \bar{t}\left(r_s \frac{\bar{a}}{\bar{s}} A - e_s S + \frac{I}{\bar{s}}\right),
\end{aligned}$$

where $\hat{d}_{y_i}(Y_i) = d_{y_i} + \tilde{d}_{y_i} Y_i$.

Choosing the constants $\bar{t}$, $\bar{y}_0$, $\bar{z}_0$, $\bar{y}_i$, $\bar{z}_i$, $\bar{a}$ and $\bar{s}$ as in Table A2 yields,

$$Y_0' = \left(\Phi_0 S - 1\right) Y_0 + \Xi_0 \tag{S.2a}$$

$$Y_i' = \left(\frac{r_i}{r_0}\Phi_i S - \frac{\hat{d}_{y_i}(Y_i) + a_i}{d_{y_0} + a_0}\right) Y_i + \Xi_i, \tag{S.2b}$$

$$\varepsilon_1 Z_0' = Y_0 - Z_0, \tag{S.2c}$$

$$\varepsilon_1 Z_i' = \frac{d_{z_i}}{d_{z_0}}\left(Y_i - Z_i\right), \tag{S.2d}$$

$$\varepsilon_2 \varepsilon_3 A' = b_{y_0} Y_0 + b_{z_0} Z_0 + \sum_{j=1}^{n}\left(b_{y_j}(Y_j) Y_j + b_{z_j} Z_j\right) - S A, \tag{S.2e}$$

$$\varepsilon_2 S' = A - S + \frac{I}{e_s \bar{s}}, \tag{S.2f}$$

where $i = 1, ..., n$ and $\varepsilon_1 = \frac{r_0}{d_{z_0}}\bar{s}$, $\varepsilon_2 = \frac{r_0}{e_s}\bar{s}$, $\varepsilon_3 = \frac{e_s}{e_a \bar{s}}$, $b_{y_0} = d_{y_0}\frac{\bar{y}_0 \bar{t}}{\bar{s}\bar{a}}\frac{d_{y_0}+a_0}{e_a}$, $b_{z_j} = d_{z_j}\frac{\bar{z}_j \bar{t}}{\bar{s}\bar{a}}\frac{d_{y_0}+a_0}{e_a}$, $b_{y_i}(Y_i) = \hat{d}_{y_i}(Y_i)\frac{\bar{y}_i \bar{t}}{\bar{s}\bar{a}}\frac{d_{y_0}+a_0}{e_a}$. Lastly, the functions Φ_i and Ξ_i correspond to scaled versions of functions φ_i and ξ_i respectively.

Time scale separation by singular geometric perturbation theory (Fenichel theory) allows for a model reduction. In particular, the full model consisting of $2n + 4$ equations can be reduced to $n + 1$ equations. The magnitudes of the ε constants are very small thus revealing the slow and fast dynamics of the model. The MPNs develop over a slow time scale and a quasi-steady state approximation (QSSA) therefore provides a suitable approximation for the modeling of MPNs. An additional advantage of the QSSA is that the number of free parameters are greatly reduced and important groupings of the parameters are revealed.

The model reduction is obtained by letting $\varepsilon \to 0$ resulting in the following algebraic equations,

$$0 = Y_0 - Z_0, \tag{S.3a}$$

$$0 = \frac{d_{z_i}}{d_{z_0}} (Y_i - Z_i), \tag{S.3b}$$

$$0 = b_{y_0} Y_0 + b_{z_0} Z_0 + \sum_{j=1}^{n} \left(b_{y_j}(Y_j) Y_j + b_{z_j} Z_j \right) - SA, \tag{S.3c}$$

$$0 = A - S + \frac{I}{e_s \bar{s}}, \tag{S.3d}$$

From Eq (S.3a) and (S.3b) it can easily be deduced that $Z_0 = Y_0$ and $Y_j = Z_j$ for $j = 1, 2, ...n$. Solving (S.3c) and (S.3d) gives

$$A = -J + \sqrt{J^2 + \sum_{j=0}^{n} 2B_j Y_j} \quad \text{and} \quad S = J + \sqrt{J^2 + \sum_{j=1}^{n} 2B_j Y_j},$$

where $J = \frac{I}{2e_s \bar{s}}$, $2B_0 = b_{y_0} + b_{z_0}$ and $2B_i = b_{y_i}(Y_i) + b_{z_i}$ for $i = 1, 2 \ldots, n$.

Inserting the found expressions in (S.2a) and (S.2b) yields the reduced MCC model,

$$Y_0' = R_0 \Phi_0 \left(J + \sqrt{J^2 + \sum_{j=1}^{n} 2B_j Y_j} \right) Y_0 - D_0 Y_0 + \Xi_0 \tag{S.4a}$$

$$Y_i' = R_i \Phi_i \left(J + \sqrt{J^2 + \sum_{j=1}^{n} 2B_j Y_j} \right) Y_i - (D_i + K_i Y_i) Y_i + \Xi_i \tag{S.4b}$$

where $R_i = \frac{r_i}{r_0}$, $D_i = \frac{d_{y_i} + a_i}{d_{y_0} + a_0}$, $K_i = \frac{\tilde{d}_{y_i}}{d_{y_0} + a_0}$ for $i = 1, 2, .., n$.

A specific choice of the inhibiting function φ is introduced. We consider the φ function proposed in [1, 4] and generalize it to the case with n malignant stem cell lines, i.e.

$$\varphi_i(y_0, y_1, ..., y_n) = \frac{1}{1 + \sum_{j=0}^{n} c_{i,j} y_j}, \tag{S.5}$$

where $c_{i,j}$ describes how cell type i is inhibited by cell type j and $c_{i,i} = 1$. The corresponding dimensionless functions are given as,

$$\Phi_i = \frac{1}{1 + \sum_{j=0}^{n} C_{i,j} Y_j}, \tag{S.6}$$

where $C_{i,j} = \frac{c_{i,j}}{c_{j,j}}$.

S.2. Sensitivity analysis

To address the sensitivity of the parameters of the MCC model we consider how the oscillations changes when changing the non-default values 10% for simulated experiment in Figure 5. In Figure S.3 the simulations are shown for the perturbed parameter values. We see the same quantitative behavior for the cell counts, i.e., oscillating cell counts. To compare the different scenarios on a single graph we compute the y_1 allele burden for the different simulations and they are depicted in Figure S.4. Figure S.4 reveals that the parameters C and K are inverse correlated, i.e., increasing K by 10% results in the same simulated allele burden as reducing C by 10%. Computing the correlation between the allele burdens give a high correlation coefficient of 0.9 confirming that the simulated allele burdens are quantitative alike. However, we note that the amplitude of the oscillations is quite sensitive to the change in the parameter values as depicted in Figure S.3. The relative percentage change of mean, amplitude and frequency for the allele burden are listed in Table 1.

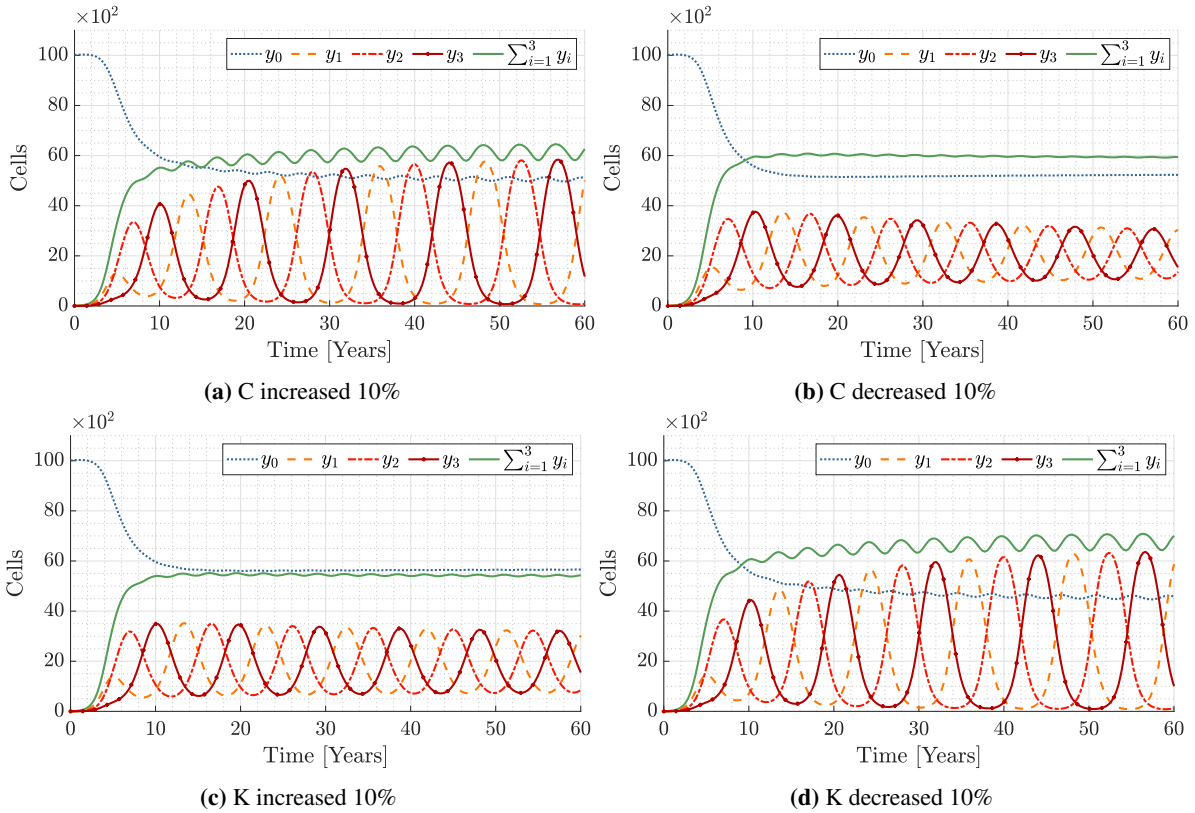

(a) C increased 10%

(b) C decreased 10%

(c) K increased 10%

(d) K decreased 10%

Figure S.3. The figure depicts the simulation scenario from Figure 5 where the non-default parameters have been increased/decreased 10% to investigate the sensitivity of the parameters. Note that the change affects the amplitude and frequency. Moreover the effect of changing K and C seems to be inverse proportional.

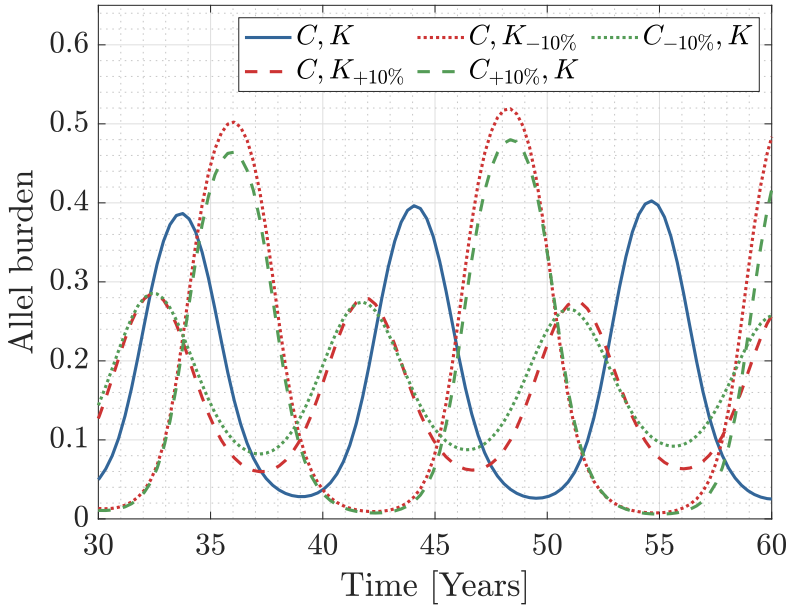

Figure S.4. Allele burden for the simulation in Figure 5 along with the allele burden for the simulations with C and K changed by 10%.

References

1. J. T. Ottesen, R. K. Pedersen, Z. Sajid, J. Gudmand-Hoeyer, K. O. Bangsgaard, V. Skov, L. Kjær, et al., Bridging blood cancers and inflammation: The reduced cancitis model, *J.Theor. Biol.*, **465** (2019), 90–108.
2. S. I. Grivennikov, F. R. Greten, M. Karin, Immunity, inflammation, and cancer, *Cell*, **140** (2010), 883–899.
3. L. M. Coussens, Z. Werb, Inflammation and cancer, *Nature*, **420** (2002), 860–867.
4. M. Andersen, Z. Sajid, R. K. Pedersen, J. Gudmand-Hoeyer, C. Ellervik, V. Skov, et al., Mathematical modelling as a proof of concept for MPNs as a human inflammation model for cancer development, *PLOS ONE*, **12** (2017), e0183620.